High-precision optical phase-locking based on wideband acousto-optical frequency shifting

Yunxiang Wang (王云祥)*, Qi Qiu (邱 琪), Shuangjin Shi (史双瑾), Jun Su (苏 君), Yun Liao (廖 云), and Caidong Xiong (熊彩东)

School of Optoelectronic Information, University of Electronic Science and Technology of China, Chengdu 610054, China

**Corresponding author: wangyunxiang@uestc.edu.cn*

Received September 22, 2013; accepted December 12, 2013; posted online January 23, 2014

We present a high-precision optical phase-locking based on wideband acousto-optical frequency shifting. Increasing the modulating bandwidth stabilizes the loop at a high loop gain, thus improving phase correction capability. An optical phase-locked loop with a wide control bandwidth is constructed. The closed-loop residual phase error is only 0.26° or smaller than $\lambda/1000$. The loop exhibits excellent correction capability for high-frequency noises. The correctable frequency range reaches 35 kHz when the noise amplitude is $\pm\lambda/2$, and becomes even wider for smaller noise amplitudes.

OCIS codes: 140.0140, 140.3298, 140.3518.
doi: 10.3788/COL201412.021402.

Active coherent beam combining (ACBC) is an important approach to scaling laser power while maintaining near-diffraction-limited beam quality, in which active phasing is one of the critical techniques[1−4]. Main phasing methods include stochastic parallel gradient descent (SPGD), dithering, and heterodyne detection[5]. In SPGD, no reference beam is required, and only one detector is used[6,7]. With this technique, Wang *et al.* realized phase-locking of two laser beams with a residual phase error of $\lambda/25$ under a laser phase noise amplitude of $\lambda/10$ and a frequency of 3 kHz[5]. Yu *et al.* realized eight-beam 4-kW coherent combining with a residual phase error of $\lambda/40$[8]. Dithering is another method that uses only a single detector, with each signal beam requiring an individual frequency or time channel. Using this technique, Ma *et al.* realized phase-locking of four beams with a residual phase error of $\lambda/40$[9]. Afterward, they achieved nine-beam 1.08-kW coherent combining with a residual phase error of $\lambda/15$[10]. In the aforementioned methods, the signal processing circuits should become more sophisticated as the number of beams increases.

Anderegg *et al.* presented the principle of heterodyne detection by using electro-optical phase modulators as phase actuators[11]. A reference beam and a photo detector array are required. Each signal beam corresponds to a processing module. The performance requirement for each module remains the same as the number of beams increases, thus endowing this technique with a relative advantage in scalability. McNaught *et al.* realized seven-beam 100-kW coherent combining of a Nd:YAG master oscillator power amplifier (MOPA) laser array with a residual phase error of $\lambda/50$[12]. Augst *et al.* proposed using an acousto-optical frequency shifter (AOFS) as the phase actuator, which provides an unlimited phase dynamic range to keep the system in phase-lock during wide range and continuous phase shifts in signal beams[13]. In their study, ACBC was achieved, but phase-locking precision was not reported, and quantitative analysis was not presented. In this letter, we analyze quantitatively the influence of modulating bandwidths of AOFS on loop performances based on phase-locked loop theory. In the experiments, expanding the modulating bandwidth results in high-precision locking with residual phase errors smaller than $\lambda/1000$ with no additional noise source in the loop. For typical phase noise amplitude and frequency range originating from fiber amplifiers, this phase-locked loop achieves a residual phase error smaller than $\lambda/500$, which can be a substantial improvement for an optical phase-locked loop (OPLL) in correcting the capability of phase noises.

The configuration of the OPLL based on an AOFS is shown in Fig. 1(a). The single-frequency narrow-width laser is generated by a nonplanar ring oscillator. The laser is split by beam splitters 1 and 2 to generate a signal and a reference beam, respectively. The reference beam is coupled with a polarization-maintaining (PM) fiber by a fiber adapter. The signal beam is focused into an 80-MHz AOFS by a lens with a 200-mm focal length. The beam waist radius in the AOFS is 0.1 mm. The first-order diffraction beam is also coupled with the PM fiber by a fiber adapter. A fiber phase modulator is used to introduce phase noises to signal beams. The signal and reference beams are mixed in the 2×2 PM fiber coupler. A PIN with 1.5-GHz bandwidth is used to detect the heterodyne signal at one output of the coupler. The heterodyne signal is mixed with an 80-MHz sine wave signal from the local oscillator (LO) to generate the phase error signal. This signal passes through the loop filter and the amplifier to generate feedback signals. The AOFS driver generates radio frequency waves, the frequency of which is controlled by the feedback signal to realize phase-locking. Augst used an AOFS with a 100-kHz modulating bandwidth. In our work, we employ an AOMO 3080-197 AOFS and an AODR 1075FM driver from CTI Inc., with a 5-MHz modulating bandwidth. Figure 1(b) shows the equivalent servo-loop diagram. The phase modulator functions as an adder for phase noise. The fiber coupler and PIN function as phase detectors.

 © 2014 Chinese Optics Letters

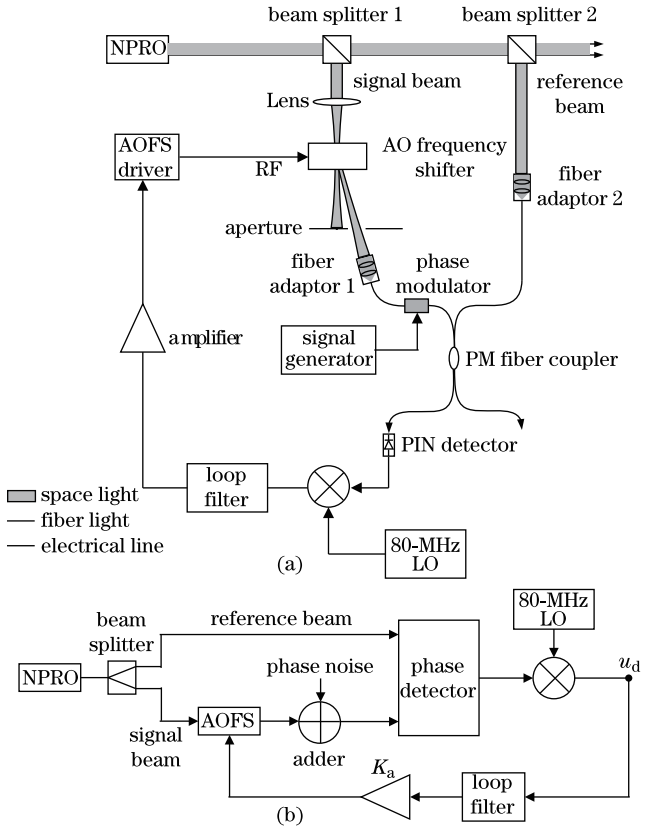

Fig. 1. (a) Schematic of the OPLL based on an AOFS and (b) its equivalent servo-loop block diagram.

The loop control bandwidth is mainly determined by the modulating bandwidth of the AOFS. The influence of the modulating bandwidth on locking performance can be demonstrated by analyzing the open-loop transfer function. When an active proportion integration filter is used as the loop filter, this function can be written as

$$H_0(f) = K\frac{1+2i\pi f\tau_2}{2i\pi f\tau_1}\frac{1}{1+if/f_H}\frac{1}{2i\pi f}\exp(-i2\pi f\tau). \quad (1)$$

The five terms on the right side represent loop gain, loop filter, low-pass filter, integrator, and loop delay, respectively. The transfer function of an AOFS is defined as the product of a low-pass filter and an integrator. $f_{\rm H}$ is a modulating bandwidth, τ is a loop delay, and τ_1 and τ_2 are the time constants of the filter. The loop gain K is the product of the amplitude of phase error signal u_d shown in Fig. 1(b), the frequency modulating coefficient of the AOFS, and the gain of the loop amplifier. K has the physical unit of rad/s. The loop phase shift is

$$Arg(H_0(f)) = -\pi + arc\tan(2\pi f\tau_2) - arc\tan(f/f_{\rm H}) - 2\pi f\tau. \quad (2)$$

The Bode criterion for stability states that a phase-locked loop (PLL) will be stable if its phase lag at the gain crossover frequency $f_{\rm gc}$ is less than 180°[14]. Thus, in the low-frequency range ($f < f_{\rm gc}$), $Arg(H_0(f))$ should be higher than -π. A necessary condition for a stable loop in the frequency range between 0 and $f_{\rm gc}$ should be

$$arc\tan(f/f_{\rm H}) + 2\pi f\tau < arc\tan(2\pi f\tau_2). \quad (3)$$

The time constant $\tau_2$is typically set to be significantly larger than the summary of τ and $1/2\pi f_{\rm H}$ to improve the stability of the loop.

According to Gardner[14], in the presence of additional components (such as a low-pass filter or delayer) in the loop, the pull-in voltage $V_{\rm d}$ is approximately equal to the pull-in voltage of the standard loop multiplied by the cosine of the added phase shift (APS), as shown in Eq. (14.6)[14]. The APS should be higher than $-\pi/2$ to obtain the correct sign for $V_{\rm d}$ and the correct lock. By contrast, an APS lower than $-\pi/2$ will result in a false $V_{\rm d}$ sign and a false lock. Therefore, pull-in frequency $f_{\rm p}$ can be estimated by

$$arc\tan(f_{\rm p}/f_{\rm H}) + 2\pi f_p\tau = \pi/2. \quad (4)$$

The pull-in frequency is typically high enough, such that the phase shift of the loop filter approaches 0. Integrating the AOFS function contributes to the phase shift of $-\pi/2$. Therefore, pull-in frequency $f_{\rm p}$ is approximately equal to the frequency at which $Arg(H_{\rm o}(f))$ reaches $-\pi$. Based on Eq. (4), the loop pull-in range widens as the loop control bandwidth increases. Thus, the pull-in ability for initial frequency difference is improved, which is important during the start of the system when the frequency difference between the LO and the heterodyne signal is comparatively large.

The calculated loop phase shift from Eq. (2) versus the frequency at different control bandwidths is shown in Fig. 2. In the calculation, the loop gain is 3.2×10^5 rad/s, and the loop delay is 300 ns. Phase shift increases at low frequency, where τ_2 exerts a major influence; and decreases at high frequency, where $f_{\rm H}$ and τ dominate the phase shift. For a stable loop, pull-in range $f_{\rm p}$ increases from approximately 200 kHz to higher than 700 kHz as $f_{\rm H}$ increases from 100 kHz to 5 MHz.

Loop delay is also crucial in loop phase shift. The pull-in range decreases as loop delay increases. As implied in Eq. (4), the increased loop delay is, to a certain extent, equivalent to decreased control bandwidth. In our loop design, loop delay is mainly caused by ultrasonic sound transiting time across the laser beam in an AOFS. The reasonable minimum transiting time is 265 ns. Total loop delay is approximately 300 ns when the delay of the light path and the electrical wire are considered.

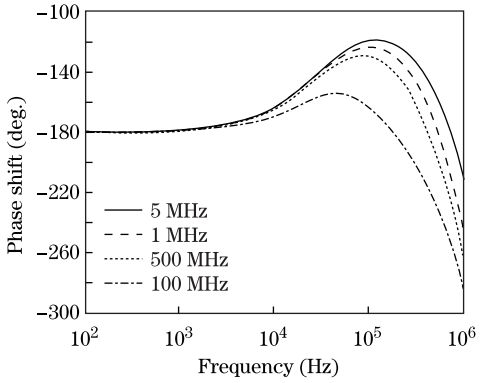

Fig. 2. Phase shift versus frequency at different modulating bandwidths.

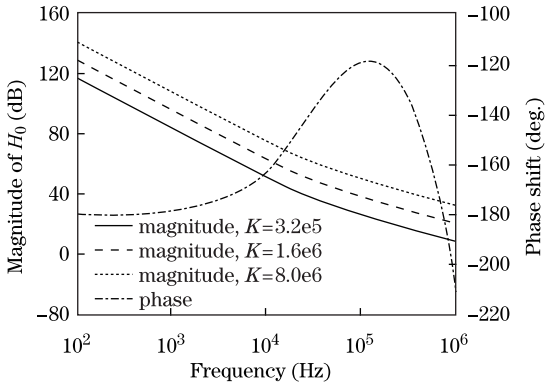

Fig. 3. Magnitude and phase shift of $H_0(f)$ versus frequency with a modulating bandwidth of 5 MHz.

The magnitude of the open-loop transfer function $20\log(|H_0(f)|)$ decreases rapidly with frequency, as shown in Fig. 3. Loop gain K is a key parameter in the loop design. With high loop gain, phase-locking precision is improved, and pull-in time is decreased. However, if K is too high, then $|H_0(f)|$ will be higher than 1 when the phase shift reaches $-\pi$. Thus, the loop becomes unstable according to Bode's rule. If the control bandwidth is broaden, then a high loop gain can be used while keeping the loop stable, as shown in Figs. 2 and 3. For a 5-MHz bandwidth, the loop gain can be set to 3.2×10^5 rad/s. In this status, the loop maintains good balance between stability and performance, with a loop phase margin of 60° and a damping factor of 0.86. By contrast, when the bandwidth is 100 kHz, K should be smaller than 8.0×10^4 rad/s to achieve a reasonable phase margin and damping factor.

The open-loop phase error signal $U_{\rm d}$ is detected at position A in Fig. 1. In the open loop status, a frequency difference occurs between the heterodyne signal and the LO signal, as shown in Fig. 4(a). The open-loop amplitude of $V_{\rm d}$ is 98 mV. As the loop closes, high precision phase-locking is realized, as shown in Fig. 4(b). The pull-in range is measured to be 700 kHz by tuning the output frequency of the AOFS driver with a step signal. The rms amplitude of $V_{\rm d}$ is measured to be 0.44 mV through signal analysis by using an oscilloscope. Compared with the open-loop amplitude of $V_{\rm d}$, the residual phase is 0.26°, which is smaller than $\lambda/1000$. During a 2-h test, the loop is kept locked, and the residual phase error exhibits no apparent variation.

The locking precision is mainly determined by correcting phase noise capability. Loop phase noise is mainly attributed to variations in the fiber refraction index. According to the measurements made by Augst, the open-loop phase noise spectrum extends to the kHz order under laboratory conditions[13]. Ideally, the loop phase noise can be corrected because the loop control bandwidth is significantly higher than the noise bandwidth and an AOFS has an unlimited dynamic range.

We conduct experiments on high-frequency noise correction to overcome high-frequency phase noises in high-power laser systems or noisy environments. Sine wave signals with different amplitudes and frequencies are applied to the phase modulator to simulate phase noise. Figure 5 shows the closed-loop residual phase error signal at the artificial noise frequencies of 1, 10, 20, and 50 kHz with a noise amplitude of $\pm\lambda/2$. The root mean square (RMS) amplitudes of the residual phase error signal are measured to be 0.6, 1.2, 4.5, and 33 mV. The corresponding residual phase errors are 0.35°, 0.7°, 2.63°, and 19.3°, respectively.

The measured residual phase errors versus the artificial noise frequencies at different noise amplitudes are shown in Fig. 6. Under the same noise amplitude, residual phase errors increase with frequency primarily because of the small $|H_0(f)|$ at high frequencies, which reduces correcting capability. Under the same noise frequency, residual phase error increases with increasing noise amplitude. This phenomenon can be mainly attributed to enhanced high-order noise harmonics that is more difficult to correct. For a typical $\lambda/10$ noise amplitude under a 3-kHz noise frequency from a fiber amplifier[5], the residual phase error is smaller than 0.4° (or $\lambda/500$) with this phase-locked loop.

The experiment al results verify that[8], in coherent combining, the loss of combining efficiency is less than 2.5% if the RMS amplitude of the residual phase error is smaller than $\lambda/40$ (or 9°). According to this criterion, the correctable frequency range is 35 kHz when the artificial noise amplitude is $\pm\lambda/2$. For smaller artificial noise amplitudes, the correctable frequency range is even wider. By contrast, the phase noise bandwidth of a typical MOPA system is within the kHz order, with a measured phase excursion of approximately $\lambda/3$ in 24 ms[13]. According to Fourier analysis, the bandwidth-limited

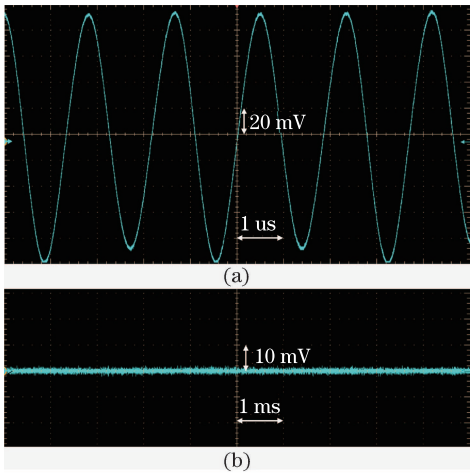

Fig. 4. Phase error signals. (a) Open loop and (b) closed loop.

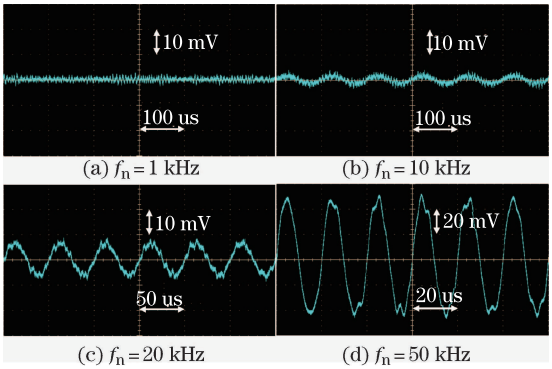

Fig. 5. Residual phase error signals at different noise frequencies with an amplitude of $\pm\lambda/2$.

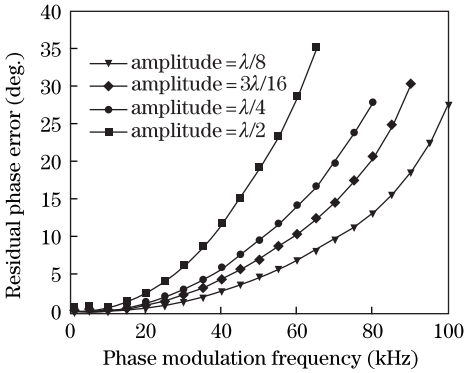

Fig. 6. Measured residual phase erros versus noise frequency at different noise amplitudes.

random phase noise can be considered as a superposition of phase fluctuations in a sine wave at different frequencies. The frequency range of intensive noise is within the kHz order for a typical fiber amplifier. Thus, the loop can correct nearly all dominant noises in the phase noise spectrum of the fiber amplifier.

Phase dynamic range is unlimited in an OPLL that employs an AOFS as the phase actuator. Thus, the loop is kept locked during continuous and large-range phase shifting. Increasing the frequency modulating bandwidth stabilizes the loop at high gains, thus improving phase-locking precision. In the experiments, an AOFS with a 5-MHz bandwidth is used in the loop. The residual phase error is 0.26° or smaller than $\lambda/1000$. The loop exhibits excellent correcting capability for high-frequency noises, which is valuable in high-power systems or systems that operate in noisy environments.

This work was supported by the Fundamental Research Funds for the Central Universities (No. ZYGX2010J059) and the National Natural Science Foundation of China (No. 61308041).

References

1. J. Bourderionnet, C. Bellanger, J. Primot, and A. Brignon, Opt. Express **19,** 17053 (2011).
2. S. J. McNaught, C. P. Asman, H. Injeyan, A. Jankevics, A. M. F. Johnson, G. C. Jones, H. Komine, J. Machan, J. Marmo, M. McClellan, R. Simpson, J. Sollee, M. M. Valley, M. Weber, and S. B. Weiss, in *Frontiers in Optics* (Optical Society of America, San Jose, California United States, 2009) FThD2.
3. P. Ma, P. Zhou, Y. Ma, R. Su, and Z. Liu, Chin. Opt. Lett. **10,** 081404 (2012).
4. X. Li, X. Dong, H. Xiao, X. Wang, and X. Xu, Chin. Opt. Lett. **9,** 101401 (2011).
5. X. Wang. P. Zhou. Y. Ma. H. Ma. X. Xu. Z. Liu. and Y. Zhao. Acta Phy. Sin. **59,** 973 (2010).
6. P. Zhou, Z. Liu, X. Wang, Y. Ma, H. Ma, X. Xu, and S. Guo, IEEE J. of Sel. Top. Quantum Electron. **15,** 248 (2009).
7. T. M. Shay, Opt. Express **14,** 12188 (2006).
8. C. X. Yu, S. J. Augst, S. M. Redmond, K. C. Goldizen, D. V. Murphy, A. Sanchez, and T. Y. Fan, Opt. Lett. **36,** 2686 (2011).
9. Y. Ma, P. Zhou, X. Wang, H. Ma, X. Xu, L. Si, Z. Liu, and Y. Zhao, Opt. Lett. **35,** 1308 (2010).
10. Y. Ma, X. Wang, J. Leng, H. Xiao, X. Dong, J. Zhu, W. Du, P. Zhou, X. Xu, L. Si, Z. Liu, and Y. Zhao, Opt. Lett. **36,** 951 (2011).
11. J. Anderegg, S. Brosnan, M. Weber, H. Komine, and M. Wickham, Proc. SPIE **4974,** 1 (2003).
12. G. D. Goodno, H. Komine, S. J. McNaught, S. B. Weiss, S. Redmond, W. Long, R. Simpson, E. C. Cheung, D. Howland, P. Epp, M. Weber, M. McClellan, J. Sollee, and H. Injeyan, Opt. Lett. **31,** 1247 (2006).
13. S. J. Augst, T. Y. Fan, and A. Sanchez, Opt. Lett. **29,** 474 (2004).
14. F. M. Gardner, *Phaselock Techniques* (3rd edn) (John Wiley & Sons, New Jersey, 2005).